JOURNAL OF MATERIALS SCIENCE 25 (1990) 3167–3172

Strain rate dependence of iodine-induced stress corrosion cracking of Zircaloy-4 under internal pressurization tests

WOO SEOG RYU*, JAI YOUNG LEE*, YOUNG HWAN KANG‡, HO CHUN SUK‡

* *Department of Materials Science and Engineering, Korea Advanced Institute of Science and Technology, PO Box 131, Cheongryang, Seoul, Korea*

‡ *Nuclear Engineering Division, Korea Advanced Energy Research Institute, PO Box 7, Daeduk Danji, Chungnam, Korea*

Pressurization tests were run on unirradiated Zircaloy-4 tubing in the pressure range of 400 to 550 MPa and temperature, 330 to 400° C. The effects of the mechanical factor on the susceptibility of Zircaloy to iodine-induced stress corrosion cracking (ISCC) were studied in terms of both time-to-failure and failure strain. The time-to-failure was related to the nth power of stress, and the failure strain was a parabolic function of the strain rate in the limited range of 10^{-7} to 10^{-4} sec^{-1}. The ISCC susceptibility was determined by the strain rate rather than the stress, and decreased with increasing test temperature. The results suggest that the film rupture step should be involved in the Zircaloy ISCC and that gas adsorption process is an important step in the overall ISCC.

1. Introduction

Models to predict the pellet-cladding interaction (PCI) failure have been suggested on the basis of the iodine-induced stress corrosion cracking (ISCC) of Zircaloy, which has been extensively studied by various testing methods including a tube internal pressurization method. The cladding failure criterion used in the PCI model is either a stress criterion based on the relationship between hoop stress and time-to-failure [1–4] or a strain rate criterion based on that between strain rate and failure strain [5, 6].

Although most of the studies have focused on the stress-based model, a few workers have reported that the strain rate is also one of the important variables in the ISCC of Zircaloy. In the constant elongation rates tests (CERT), gaseous iodine reduced the load-carrying capacity of irradiated Zircaloy-2 [7, 8] and ISCC susceptibility of Zircaloy was dependent on the strain rate [9, 10]. In the internal pressurization tests of the tube, the relationship between ISCC susceptibility of Zircaloy and strain rate has also been reported. Peehs *et al.* [11] showed that the uniform elongation was dependent on the strain rate in the iodine atmosphere and Jones *et al.* [12] recommended that the hoop strain rate should be more influential in determining the time-to-failure in ISCC tests than either the hoop stress or strain. Wood and Hardy [13] suggested the threshold strain rate below which ISCC of Zircaloy does not occur. In addition, Williford [6] has developed a strain rate-based PCI model.

The experimental data, however, on the strain rate dependence of the Zircaloy ISCC are not available and the relation between the stress-based criterion and the strain rate-based one has not been studied. Moreover, the SCC mechanism has not been understood with respect to the strain rate dependence of Zircaloy ISCC.

In this work, the strain rate dependence of ISCC susceptibility of Zircaloy-4 tubing is intensively investigated using internal pressurization tests and an ISCC mechanism is discussed in terms of the strain rate.

2. Experimental details

Details of the experimental procedures have been described previously [14] and will not be repeated here. All of the tests were conducted on nuclear grade, unirradiated Zircaloy-4 tubing with an outside diameter of 13.08 mm and a wall thickness of 0.42 mm. Test specimens about 100 mm long were cut from the cladding tube. A high purity argon gas was used in the tube internal pressurization system. A given amount of iodine was loaded into the specimen using a glass ampule.

The values of the nominal hoop stress were calculated as

$$\sigma = \frac{R_o^2 + R_i^2}{R_o^2 - R_i^2} \times P \quad (1)$$

where R_i and R_o are the inside and outside radii, respectively, of the tubing specimen and P the internal gas pressure. The failure strain was calculated as

$$\varepsilon_f = \frac{R_f - R_o}{R_o} \quad (2)$$

where R_f is the outside radius of the tubing after failure. When an axial split failure occurred, the

0022–2461/90 $03.00 + .12

failure strain was not calculated, because R_f could not be measured. The average strain rate was calculated as

$$\varepsilon_m = \varepsilon_f / t_f \quad (3)$$

where t_f is the time-to-failure.

The average strain rate gives a measure of the mean plastic strain rate, which was faster than the secondary creep rate but slower than the primary creep rate during a constant load test as shown in the previous paper [14]. At a failure strain above 10%, the average strain rate did not have a significant meaning, because the tube specimen resulted in excessive local deformation.

To examine the SEM fractographs, the failure section was broken open in liquid nitrogen by bending the half ring which had been cut from the failed specimen.

3. Results

3.1. Relationship between time-to-failure and stress

Figure 1 shows the time-to-failure as a function of hoop stress at an iodine concentration of $2\,mg\,cm^{-2}$ and a temperature of 330° C. The time-to-failure increased with decreasing hoop stress, in agreement with others [1, 5, 12–16]. Using the least-square method, a relationship between hoop stress and time-to-failure was obtained as Equation 4 in the range of 400 to 500 MPa in which ISCC apparently occurred.

All of the specimens showed two types of failure, pinhole and axial-split. An axial split-type failure, in general, has been observed at high stresses [5, 15], but in this work it was also observed at low stresses with the long time-to-failure, indicating the loss of effectiveness of iodine as a SCC agent at low stresses. The threshold stress is suggested to be located below

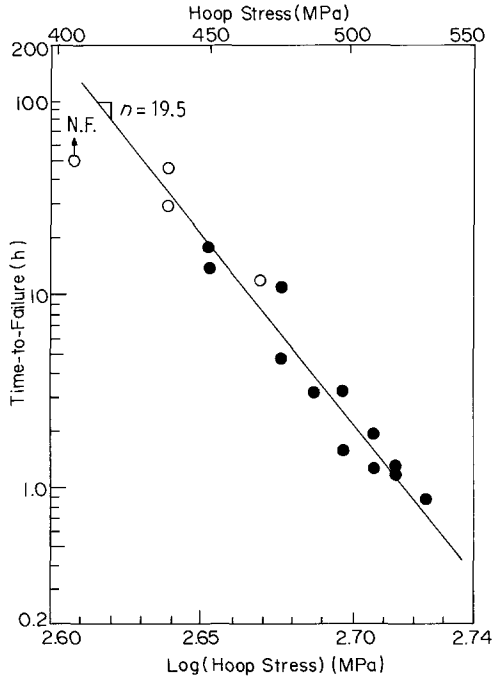

Figure 1 Time-to failure as a function of hoop stress at 603 K. (○ = axial-split failure, ● = pinhole failure, NF = non-failure), iodine concentration = $2\,mg\,c^{-2}$.

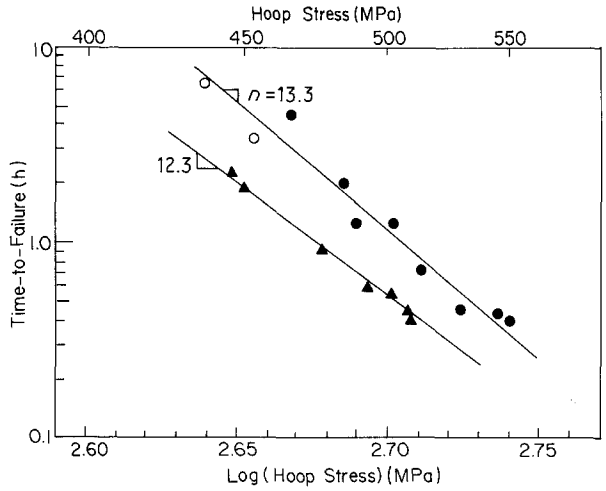

Figure 2 Time-to-failure as a function of hoop stress at 633 K. (○△, axial-split failure, ●▲, pinhole failure), (Iodine concentration ○●, $2\,mg\,cm^{-2}$, △▲, $4\,mg\,cm^{-2}$).

437 MPa in this work because the time-to-failure increased rapidly and the failure mode was an axial-split type below 437 MPa, indicating that the SCC susceptibility was significantly reduced with decreasing hoop stress.

Figures 2 to 4 show the time-to-failure as a function of hoop stress at 360, 380, and 400° C, respectively. The overall behaviours were similar to the data of 330° C, but the time-to-failure decreased in a given hoop stress with increasing temperature. Least-square fittings of the data yield the relationship

$$t_f = A\sigma^{-n} \quad (4)$$

The values of constants A and n are summarized in Table I. The stress exponent, n, which represents the slope of curve in the figure, decreased from 19.5 to 7 with increasing temperature at a given iodine concentration of $2\,mg\,cm^{-2}$, a decrease from 17 to 6 with increasing iodine concentration at a temperature of 400° C. These results are similar to those of Shann and Olander [15], in which the time-to-failure varied as a function of the eighth power on stress at 0.01 torr iodine pressure and 300° C.

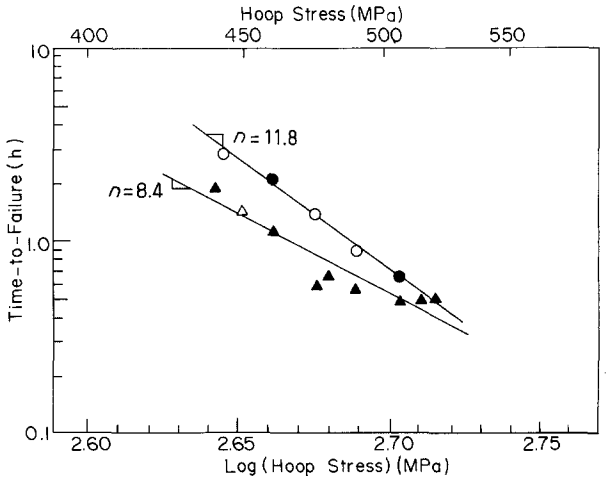

Figure 3 Time-to-failure as a function of hoop stress at 653 K. (○△, axial-split failure, ●▲, pinhole failure), (Iodine concentration ○●, $2\,mg\,cm^{-2}$, △▲, $4\,mg\,cm^{-2}$).

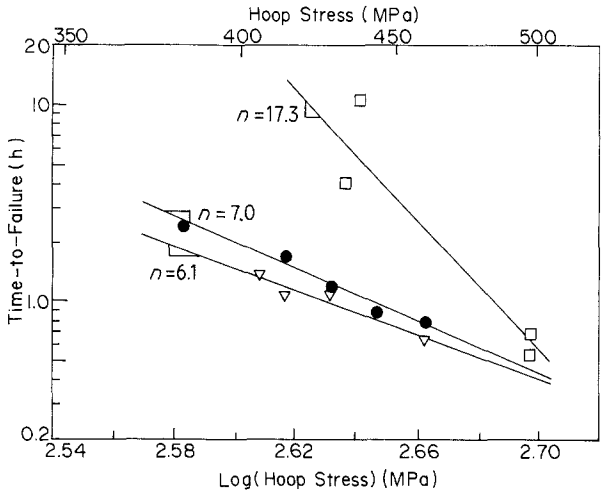

Figure 4 Time-to-failure as a function of hoop stress at 673 K. (□, ▽, axial-split failure, ●, pinhole failure; iodine concentration: □ 1 mg cm^{-2}, ●, 2 mg cm^{-2}, ▽, 6 mg cm^{-2}).

3.2. Relationship between failure strain and strain rate

The strain rate in this work was defined as the average strain rate calculated from Equation 3, and was a function of the hoop stress as shown in Fig. 5. Least-square fittings yield Equation 5, similar to the creep equation of Zircaloy [17].

$$\dot{\varepsilon}_m = C\sigma^n \quad (5)$$

The stress exponent, n, is dependent on both temperature and iodine concentration, and increased in the range of 6 to 17 with decreasing temperature at the same iodine concentration.

Figure 6 shows the failure strain as a function of strain rate at the iodine concentration of 2 mg cm^{-2} and the test temperature of 330° C. Data points on the strain rate curve correspond to the stresses of 400 to 530 MPa in Fig. 1, and are in the range of 10^{-7} to 10^{-4} sec^{-1}, which is the range of the tensile strain rate to promote SCC for many metal systems [18]. In the figure the dependence of the failure strain on the strain rate is clear, and the failure strain shows a minimum of 2.8% at an intermediate strain rate of 6.7×10^{-6} sec^{-1}. Below 2×10^{-6} sec^{-1}, because most specimens failed in an axial-split mode, the failure strain could not be measured. Therefore, the data in the figure are not real values but nominal ones inferred from the failure strains which were measured in part out of axial-split of tube. The threshold strain rate [5, 12] above which ISCC would occur was not clearly defined in this result, but it is assumed to be a strain rate at which the failure strain of ISCC equals that of burst tests. Similar results on the strain rate dependence of the Zircaloy SCC have been reported. Wood *et al.* [13] and Jones *et al.* [5, 12] have reported the threshold strain rate of an order of about 10^{-7} sec^{-1}. Peehs *et al.* [11] showed a minimum strain at a strain rate of 1.7×10^{-7} sec^{-1}.

TABLE I Values of constant A and stress exponent n in the equation $t_f = A\sigma^{-n}$

Temperature (° C)	Iodine concentration (mg cm^{-2})	A	n
330	2	8.2×10^{52}	19.5
360	2	9.0×10^{35}	13.3
360	4	7.0×10^{32}	12.3
380	2	3.8×10^{31}	11.8
380	4	2.4×10^{22}	8.4
400	1	2.3×10^{46}	17.3
400	2	3.5×10^{18}	7.0
400	6	1.2×10^{16}	6.1

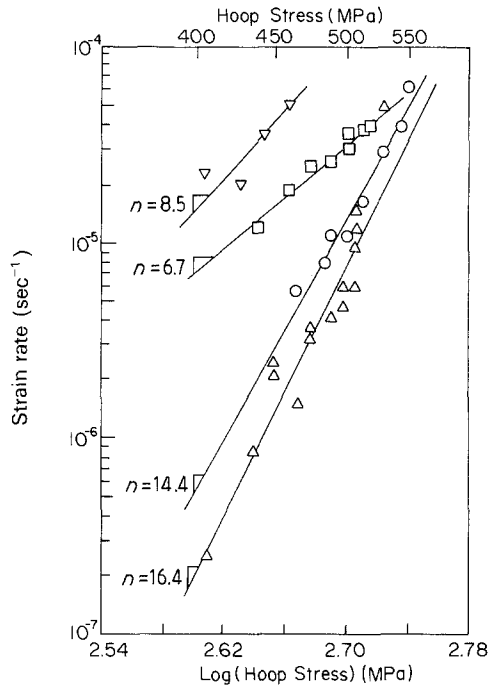

Figure 5 Variation of average strain rate with hoop stress. (▽ = 400° C, 2 mg cm^{-2}; □ = 380° C, 4 mg cm^{-2}; ○ = 360° C, 2 mg cm^{-2}; △ = 330° C, 2 mg cm^{-2})

Figure 7 shows the failure strain as a function of strain rate at 360 to 400° C. In the figure, 380° C data were measured at an iodine concentration of 4 mg cm^{-2} because most specimens at 2 mg cm^{-2} failed in an axial-split mode, and the strain rates at 400° C are the nominal values and have some discrepancy with real values, because specimens failed in an excessive local deformation above 10% of failure strain. Although the dependence of failure strain on the strain rate at 360 to 400° C shows a similar trend with that of 330° C, the overall failure strain increased with

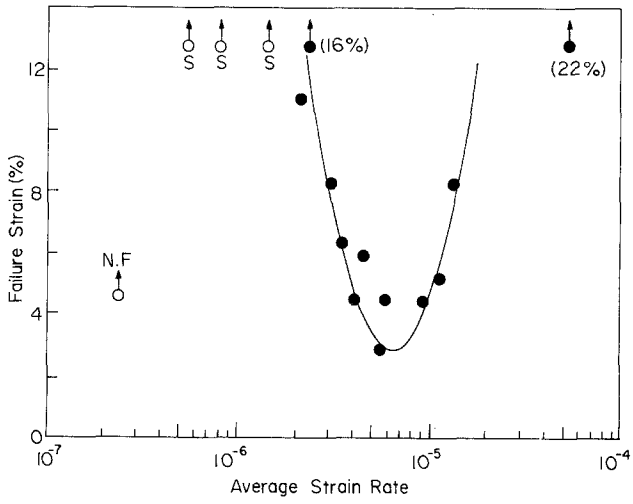

Figure 6 Variation of failure strain with strain rate at 603 K. (open mark = axial-split failure, NF = non-failure).

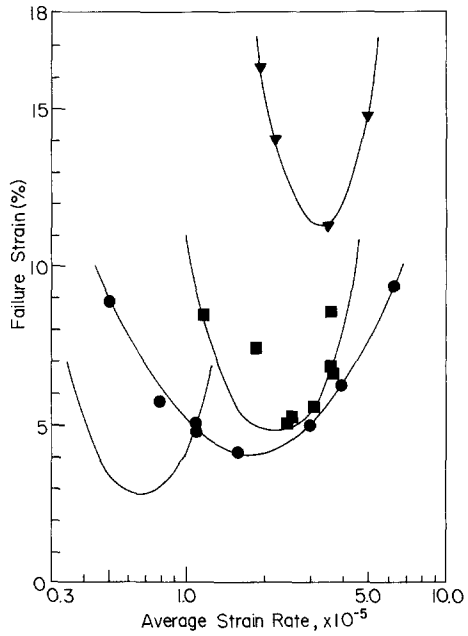

Figure 7 Affect of test temperature on the ISCC behaviour. (▼ = 400° C, 2 mg cm^{-2}; ■ = 380° C, 4 mg cm^{-2}; ● = 360° C, 2 mg cm^{-2}; – 330° C, 2 mg cm^{-2}).

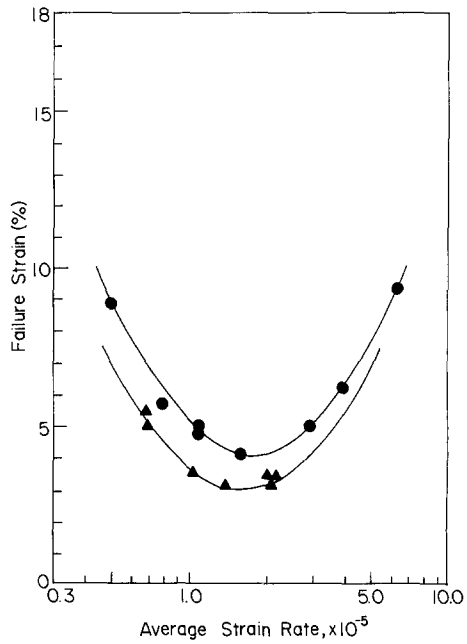

Figure 8 Affect of iodine concentration of the ISCC behaviour at 633 K. (● = 2 mg cm^{-2}, ▲ = 4 mg cm^{-2}).

temperature and the axial-split failure became more predominant. Fig. 8 shows the dependence of failure strain on the iodine concentration. The failure strain increased with decreasing iodine concentration at a given strain rate but the strain rates at the minimum strain rate were almost the same both in 2 mg cm^{-2} and in 4 mg cm^{-2} at 360° C, in agreement with the results of Peehs *et al.* [11].

The best fit curves of failure strain were obtained as a function of strain rate: i.e.

$$\varepsilon_f = A(\log \dot{\varepsilon}_m + B)^2 + C \quad (6)$$

constants A, B and C are summarized in Table II. The strain rate at a minimum of failure strain, which is represented by a constant B, depends on temperature as

$$\dot{\varepsilon}_{min} = 27.5 \exp(-9.15/RT) \quad (7)$$

The failure strain at the minimum failure strain, which is represented by a constant C, is increased with increasing test temperature at a given iodine concentration, which is consistent with the data of Jones *et al.* [5, 12]. Considering the ductility minimum phenomenon of Zircaloy-4 in this temperature range [19, 20], the ISCC susceptibility, which can be represented by the ratio of failure strains under an iodine atmosphere and that of an inert one, should be reduced as temperature increased.

TABLE II Values of constant A, B and C in the equation $\varepsilon_f = A(\log \dot{\varepsilon}_m + B)^2 + C$.

Temperature (° C)	Iodine concentration (mg cm^{-2})	A	B	C
330	2	49.9	5.17	2.8
360	2	16.3	4.75	4.1
360	4	15.7	4.79	3.0
380	4	56.0	4.66	4.4
400	2	99.7	4.48	11.2

3.3. Fractographs

The typical fractographs with various strain rates at 2 mg cm^{-2} and 360° C are shown in Fig. 9. Fig. 9a, failed at a fast strain rate of 6.4 × 10^{-5} sec^{-1} with a large failure strain of 9.2%, shows a quasi-cleavage mode with a number of tearing ridges but not a ductile mode with microvoid coalescence. Fig. 9b, failed at a intermediate strain rate of 1.6 × 10^{-5} sec^{-1} with a small failure strain of 4.2%, shows the typical SCC fractograph, with obvious tearing ridges produced by tearing two breaches of cracks in the bottom of the figure. Fig. 9c, failed at a low strain rate of 5.3 × 10^{-6} sec^{-1} with a large failure strain of 8.8%, shows the quasi-cleavage mode similar to Fig. 9b with distinct tearing ridges.

Fig. 10 shows the fractographs which failed with an extremely large failure strain at 2 mg cm^{-2} and 330° C. Although a quasi-cleavage failure was observed at the intermediate strain rate with a small failure strain as shown in Fig. 10b, a ductile failure with microvoid coalescence, as shown in Figs 10a and 10b, was observed in the extreme conditions of both fast and slow strain rates with very high failure strains.

These results back up the above results, which indicated that Zircaloy is susceptible to SCC in the limited ranges of strain rate.

4. Discussion

The ISCC susceptibility of Zircaloy-4 has been represented by the relationship between the time-to-failure and stress [1–4]. Recently, the strain rate was known to be one of the important factors, and the failure strain was well described as a function of strain rate in this work. In addition, the stress dependence of the time-to-failure could be explained by the relationship between the failure strain and the strain rate. That is, the time-to-failure was related to the strain rate as

$$t_f \propto 1/\dot{\varepsilon}_m \quad (8)$$

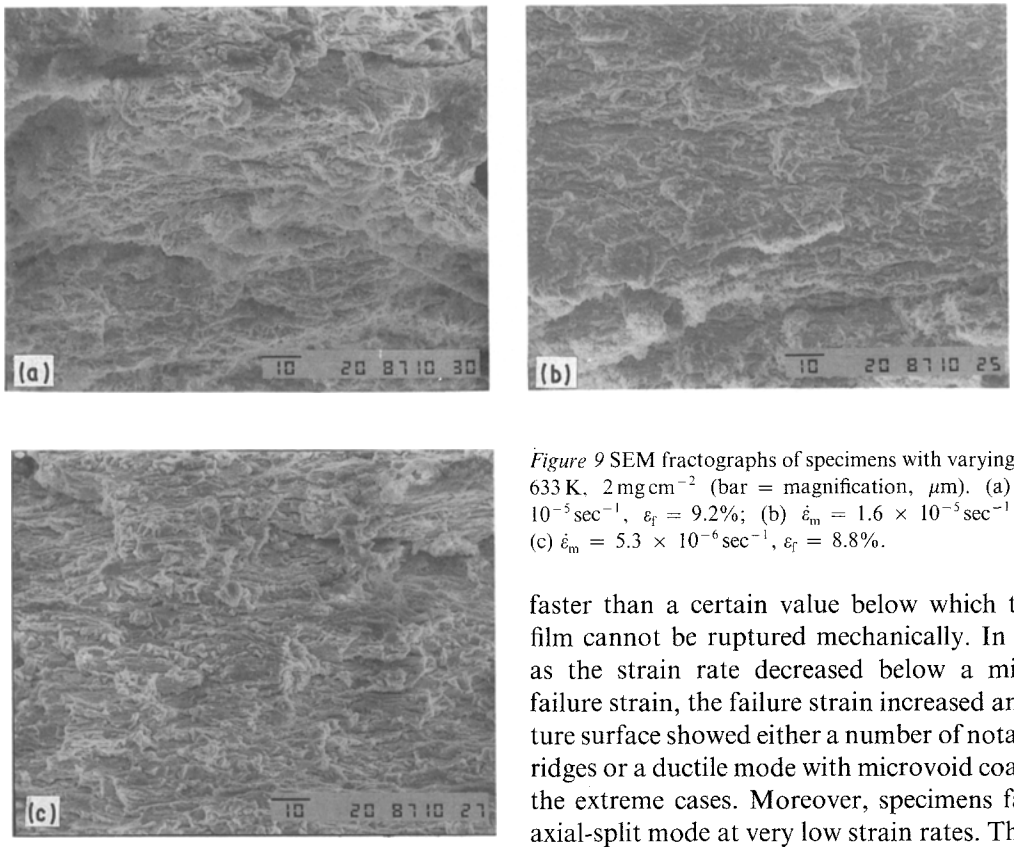

Figure 9 SEM fractographs of specimens with varying strain rate at 633 K, 2 mg cm^{-2} (bar = magnification, μm). (a) $\dot{\varepsilon}_m = 6.4 \times 10^{-5}$ sec^{-1}, $\varepsilon_f = 9.2\%$; (b) $\dot{\varepsilon}_m = 1.6 \times 10^{-5}$ sec^{-1}, $\dot{\varepsilon}_f = 4.2\%$; (c) $\dot{\varepsilon}_m = 5.3 \times 10^{-6}$ sec^{-1}, $\varepsilon_f = 8.8\%$.

Substituting Equation 6 into Equation 9 yields

$$t_f \propto \sigma^{-n} \tag{9}$$

Equation 9 is consistent with Equation 4. The stress exponents obtained from the relationships between the time-to-failure and stress, which varied from about 6 at 400° C to about 20 at 330° C, were relatively consistent with those between the strain rate and stress.

The ISCC susceptibility of Zircaloy could be represented by the relationship between failure strain and strain rate. Failure strains were related to the second power on the strain rate as shown in Figs 6 and 7, and a minimum is observed in the plot at an intermediate strain rate. It suggests that the rupture of solid film may be involved in the ISCC of Zircaloy [5, 12, 21]. Iodine reacts upon zirconium to produce gaseous zirconium tetraiodides and solid iodides [22–24]. Zirconium tetraiodide is a candidate for corrodant to cause the ISCC of Zircaloy. Thus, the reaction between the zirconium tetraiodide and the Zircaloy metal surface is one of the significant steps in the ISCC mechanism. By the way, zirconium tetraiodide forms the adsorption equilibrium on the metal surface and reacts upon the zirconium metal to form zirconium triiodide below 530° C which is a dense solid film [25]. Therefore, it seems that solid film involved in ISCC of Zircaloy should be the dense film of zirconium triiodide, but further studies will be necessary to identify this.

If the solid film was involved in the ISCC of the Zircaloy, the surface film should be ruptured mechanically and the fresh metal exposed to the corrosive environment in order to propagate the stress corrosion cracks. The strain rate should be, therefore, faster than a certain value below which the surface film cannot be ruptured mechanically. In this result, as the strain rate decreased below a minimum of failure strain, the failure strain increased and the fracture surface showed either a number of notable tearing ridges or a ductile mode with microvoid coalescence in the extreme cases. Moreover, specimens failed in an axial-split mode at very low strain rates. This suggests that there is a threshold strain rate above which SCC will occur [5, 12, 13].

Above the threshold strain rate, the corrodants should be adsorbed on the fresh metal surface to embrittle Zircaloy by reducing the surface energy or by weakening the metal bonding strength [6, 22, 23]. The adsorption rate is generally expressed by Equation 10 and increases with temperature [25]

$$d\theta/dt = A(1 - \theta)P \exp(-Q_a/RT) \tag{10}$$

where θ is coverage, A a constant, P the gas pressure and Q_a the activation energy for condensation. Assuming that the embrittlement factor due to adsorption is a function of coverage [6], it increases with increasing temperature. The formation rate, however, of the solid film which protects the adsorption of zirconium tetraiodides on the fresh metal surface also increases with temperature. Therefore, the strain rate at which the failure strain shows a minimum, resulting from the competition between the embrittlement due to the adsorption and the protection by the solid film, increases with increasing temperature as shown in Fig. 7.

The surface concentration due to adsorption, γ, can be expressed by Equation 12 and decreases with temperature [25]

$$\gamma = z\tau_o \exp(Q/RT) \tag{11}$$

where z is the collision factor, τ_o the time of stay of the molecule on the surface at $Q = 0$, and Q the interaction energy. The embrittlement factor, which is a function of surface concentration, decreases with increasing temperature at a given iodine concentration. Thus the minimum failure strain, depending on the embrittlement factor, increases with increasing temperature as shown in Fig. 7.

These results suggest that the strain rate rather than

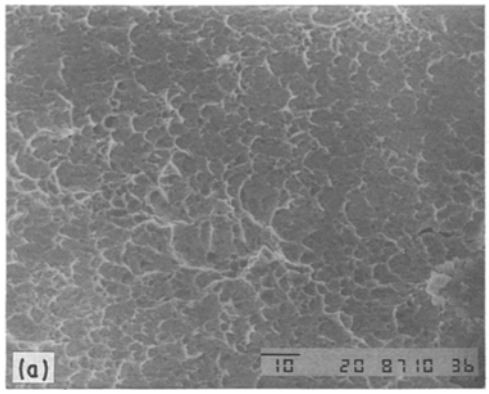

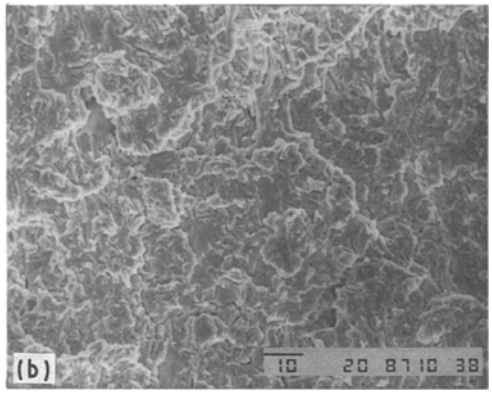

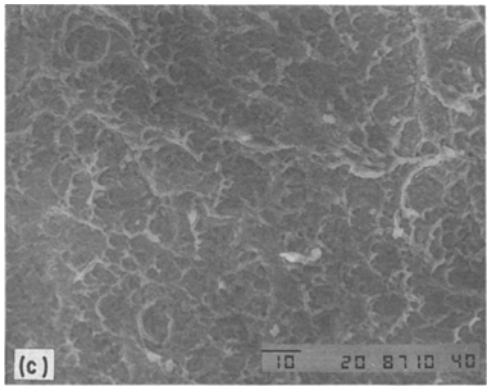

Figure 10 SEM fractographs of specimen with varying strain rate at 603 K, 2 mg cm^{-2} (bar = magnification, μm). (a) $\dot{\varepsilon}_m = 5.4 \times 10^{-5}$ sec^{-1}, $\varepsilon_f = 22\%$; (b) $\dot{\varepsilon}_m = 3.6 \times 10^{-6}$ sec^{-1}, $\varepsilon_f = 6.3\%$; (c) $\dot{\varepsilon}_m = 2.5 \times 10^{-6}$ sec^{-1}, $\varepsilon_f = 16\%$.

either stress or strain is a more important mechanical variable in the internal pressurization tests of the ISCC of Zircaloy. In order to clarify the strain rate dependence of the Zircaloy ISCC, further investigations will be necessary through the constant elongation rate test.

5. Conclusions

The conclusions are as follows

(1) The time-to-failure in the Zircaloy ISCC was related to the nth power on stress and the stress exponent varied from about 6 at high temperatures to about 20 at low temperatures.

(2) The failure strain in the Zircaloy ISCC was a parabolic function of strain rate. Both the strain rate at a minimum of failure strain and the minimum failure strain increased with increasing temperature.

(3) Strain rate rather than stress was more influential in determining the susceptibility in the Zircaloy ISCC tests.

(4) The film rupture step was involved in the Zircaloy ISCC, which occurred only within a limited range of strain rates. A gas adsorption process was an important step in the overall ISCC of Zircaloy.

Acknowledgements

The authors are indebted to Mr S. J. Park for assistance in running the experiments. Thanks are also due to Mr K. N. Joo and Dr S. M. Oh for discussing the work.

References

1. J. T. A. ROBERTS, R. L. JONES, D. CUBICCIOTTI, A. K. MILLER, H. F. WACHOB, E. SMITH and F. L. YAGGEE, in Zirconium in the Nuclear Industry ASTM STP 681 (American Society for Testing and Materials, Philadelphia, 1979) pp. 285–305.
2. A. K. MILLER, K. D. CHALLENGER and A. TASOOJI, Electric Power Research Institute Report EPRI-NP-1798 (1981).
3. R. F. MATTAS, F. L. YAGGEE and L. A. NEIMARK, in (American Nuclear Society, Oregon, 1979), Topical Meeting on Light Water Reactor Fuel Performance, Portland, Oregon, 1979), pp. 128–140.
4. P. H. KREYNS, G. L. SPAHR and J. E. McCAULEY, *J. Nucl. Mater.* **61** (1976) 203.
5. R. L. JONES, F. L. YAGGEE, R. A. STOEHR and D. CUBICCIOTTI, *ibid* **82** (1979) 26.
6. R. E. WILLIFORD, *Nucl. Eng. Des.* **78** (1984) 23.
7. D. S. TOMALIN, ASTM STP 633 (American Society for Tesing and Materials, Philadelphia, 1977) pp. 557–572.
8. D. LEE and R. B. ADAMSON, *ibid.* pp. 385–401.
9. L. F. COFFIN, ASTM STP 681 (American Society for Testing and Materials, Philadelphia, 1979) pp. 72–87.
10. K. UNE, *J. Nucl. Sci. Technol.* **16** (1979) 660.
11. M. PEEHS, H. STEHLE and E. STEINBERG, ASTM STP 681 (American Society for Testing and Materials, Philadelphia, 1979) pp. 244–260.
12. R. L. JONES, D. CUBICCIOTTI and B. C. SYRETT, *J. Nucl. Mater* **91** (1980) 277.
13. J. C. WOOD and D. G. HARDY, in: Proceedings ANS Topical Meeting on Light Water Reactor Fuel Performance, (American Nuclear Society, St. Charles, Illinois), 1977, p. 315.
14. W. S. RYU, Y. H. KANG and J. Y. LEE, *J. Nucl. Mater.* **152** (1988) 194.
15. S. H. SHANN and D. R. OLANDER, *ibid* **113** (1983) 234.
16. B. COX and J. C. WOOD "Corrosion Problems in Energy Conversion and Generation", edited by C. S. Tedman, Jr. (Electrochemical Society, New York, 1974) p. 275.
17. D. L. DOUGLASS, in "The Metallurgy of Zirconium, Atomic Energy Review Supplement" 1971 (IAEA, 1971) pp. 265–274.
18. R. N. PARKINS, ASTM STP 665 (American Society for Testing and Materials, Philadelphia, 1979) pp. 5–25.
19. S. I. HONG, W. S. RYU and C. S. RIM, *J. Nucl. Mater.* **116** (1983) 314.
20. *Idem, ibid* **120** (1984) 1.
21. R. P. GANGLOFF, D. E. GRAHAM and A. W. FUNKENBUSCH, *Corrosion-NACE* **35** (1979) 316.
22. D. CUBICCIOTTI, R. L. JONES and B. C. SYRETT, ASTM STP 754 (American Society for Testing and Materials, Philadelphia, 1983) pp. 146–157.
23. P. HOFMANN and J. SPINO, *J. Nucl. Mater.* **114** (1983) 50.
24. H. FEUERSTEIN, Oak Ridge National Laboratory Report ORNL-4543 (1970).
25. A. W. ADAMSON, "Physical Chemistry of Surfaces" (John Wiley & Sons, New York, 1982) pp. 517–616.

Received 9 February
and accepted 24 August 1989